Atmospheric Research 287 (2023) 106698

Contents lists available at ScienceDirect

Atmospheric Research

journal homepage: www.elsevier.com/locate/atmosres

Microwave radiometer, sun-photometer and GNSS multi-comparison of integrated water vapor in Southwestern Europe

Javier Vaquero-Martínez [a,*], Manuel Antón [b], Maria João Costa [c], Daniele Bortoli [c], Francisco Navas-Guzmán [d,e], Lucas Alados-Arboledas [d,e]

[a] Departamento de Didáctica de las Ciencias Experimentales y las Matemáticas, Instituto Universitario de Investigación del Agua, Cambio Climático y Sostenibilidad (IACYS), Universidad de Extremadura, Cáceres, Spain
[b] Departamento de Física, Instituto Universitario de Investigación del Agua, Cambio Climático y Sostenibilidad (IACYS), Universidad de Extremadura, Badajoz, Spain
[c] Earth Remote Sensing Laboratory (EaRSLab), Institute of Earth Sciences and Physics Department, Universidade de Évora, Portugal
[d] Applied Physics Department, University of Granada, Granada, Spain
[e] Andalusian Institute for Earth System Research (IISTA-CEAMA), 18006 Granada, Spain

ARTICLE INFO

Keywords:
Water vapor
Sun-photometer
Microwave radiometer
GNSS
Southwestern Europe
Iberia

ABSTRACT

This work presents a comparison of integrated water vapor (IWV) data recorded from microwave radiometer (MWR) and sun-photometer (SP) using global navigation satellite system (GNSS) IWV as reference in five mid-latitude sites of Portugal and Spain (2003–2021). A very high correlation is obtained for both instruments (R^2 between 0.94 and 0.98), although, while MWR shows a wet bias, SP exhibits a dry one. In addition, a dependence of mean bias error (MBE) and standard deviation (SD) on IWV has been observed, increasing (larger discrepancies) both indices as IWV increases. The solar zenith angle (SZA) dependence is also studied, finding slightly larger discrepancies for the MWR than for SP in comparison with GNSS for very high values of SZA. Finally, a marked seasonal dependence is observed for SP-GNSS differences, modulated by the IWV dependence explained above. In contrast, the seasonal dependence for MWR is quite weaker than it is for SP. Therefore, in spite of the excellent agreement found among the different instruments, it is recommended that: i) the dependence with IWV be studied and corrected to further increase the performance of the instruments, and ii) metadata be used to filter out situations in which the instrument cannot operate properly.

1. Introduction

Water vapor is well known as a trace gas with a paramount importance in many atmospheric processes. It is crucial to the water cycle and it is also the main absorber of infrared radiation, which makes it the most important natural greenhouse gas (Myhre et al., 2013). Its role in the climate system is considered as a positive feedback (Colman, 2003; Colman, 2015).

However, monitoring water vapor is a difficult task due to the high variability of its concentration in both the temporal and spatial regimes. It is crucial for researchers to have coincident instrumentation that allows comparisons among them, and to increase sampling. Although atmospheric water vapor concentration can be measured using very different variables (relative humidity, specific humidity, profiles, superficial variables, integrated, …), IWV is a very common choice. This variable is defined as the integration, in the vertical path, of the volumetric concentration of water vapor as a function of height. In such case, the units are those of superficial concentration (g cm^{-2} or kg m^{-2}). However, it can be seen in terms of precipitable water vapor, which represents the height that the water vapor in an atmospheric column would reach in a vessel of the same cross section as the column if all of it condensated. In this case, the units are those of length (cm or mm), equivalent to those of superficial concentration assuming that the density of liquid water is 1 g cm^{-3}.

Among other instruments, ground-based GNSS stations provide high quality data with high temporal resolution, allowing continuous monitoring under any sky condition (Vaquero-Martínez and Antón, 2021). Moreover, its use for geodetic purposes and inexpensive maintenance have allowed the creation of dense networks. Particularly, Nevada Geodetic Laboratory (Blewitt et al., 2018) has compiled a huge, world-

* Corresponding author at: Departamento de Física, Instituto Universitario de Investigación del Agua, Cambio Climático y Sostenibilidad (IACYS), Universidad de Extremadura, Badajoz, Spain.
E-mail address: javier_vm@unex.es (J. Vaquero-Martínez).

https://doi.org/10.1016/j.atmosres.2023.106698
Received 25 November 2022; Received in revised form 30 January 2023; Accepted 27 February 2023
Available online 8 March 2023

wide data-set of around 1300 GNSS stations and processed their data to retrieve the IWV. This IWV data-set has already been used for validation of other products by Yu et al. (2021). In that work, both GNSS and satellite data-sets were used as reference to validate numerical weather models, with similar conclusions.

Another interesting instrumentation for monitoring the atmosphere are sun-photometers (SP). The Aerosol Robotic Network (AERONET) provides a very standardized, high-quality network of SP with world-wide coverage and freely available data. Although their main interest is on aerosols, IWV is retrieved as well (Holben et al., 1998). AERONET counts with more than 800 stations worldwide, now reprocessed with a new version of the algorithm (3.0, see Sinyuk et al., 2020) and three quality levels (level 1.0 for raw data, cloud-screened as level 1.5, and quality assured data in level 2.0).

In addition, the MWR are instruments that have been traditionally used to retrieve water vapor and liquid water in the atmosphere, as they can measure brightness temperature in bands of the microwave spectrum that are affected by the presence of water masses (see, for example, Turner et al., 2007).

The study region of this work is the south-west of Europe, including the Iberian Peninsula and the Azores archipelago. This region presents different climatological scenarios (Atlantic, Continental, Mediterranean), which is useful since it allows for comparing instrument behavior under different conditions.

This paper is organized as follows: Section 2 presents the data used in this study. Then, Section 3 draws the methodological details of the comparison. After that, Section 4 presents and discusses the results of this work, and finally the conclusions are drawn in Section 5.

2. Data

2.1. Microwave radiometer measurements

MWRs provide brightness temperature measurements in microwave spectral bands that depend on atmospheric humidity and can thus be used to retrieve IWV. Two similar microwaves radiometers (RPG-HATPRO, Radiometer Physics GmbH) are operated at Evora and Granada stations. This instrument provides very accurate values of Liquid Water Path (LWP) and IWV with a high temporal resolution (1 s). Measurements in the bands 22 to 31 and 51 GHz to 58 GHz make it possible to retrieve humidity and temperature profiles with this radiometer (Rose et al., 2005).

HATPRO measures the sky brightness temperature at six elevation angles 90:0, 42:0, 30:0, 19:2, 10:2 and 5:4° corresponding to 1:0, 1:5, 2:0, 3:0, 5:6 and 10:6 air masses in a continuous and automated way with a radiometric accuracy between 0.3 and 0.4 K root mean square error at 1.0 s integration time. Whereas the first band provides highly accurate information of humidity and cloud liquid water content (Löhnert and Crewell, 2003), the second band contains information about the tropospheric vertical structure of the temperature due to the homogeneous mixing of O2 (Crewell and Lohnert, 2007). HATPRO uses two filter banks to detect the radiation coming from both bands in parallel. For the product of interest in this study, IWV information is obtained using a neural network approach with the brightness temperature as input. The manufacturer reports a root-mean-square accuracy of ± 0.2 kg m^{-2} and a random error of 0.05 kg m^{-2} root-mean-square (online athttps://www.radiometer-physics.de; last accessed 31/10/2022).".

The Eastern North Atlantic (ENA) measurement site from the Atmospheric Radiation Measurement (ARM) user facility, located on Graciosa Island in the Azores archipelago, operates a 3-channel MWR (MWR3C). It provides brightness temperature measurements in 3 spectral channels (23:8, 30 and 89 GHz), which are sensitive to the presence of liquid water and IWV (Cadeddu et al., 2013). ARM provides IWV retrieval from MWR3C using a neural network algorithm, with an estimated uncertainty of 0.05 cm (Cadeddu, 2021). The location of the three sites along with the rest of operation positions are specified in Table 1.

2.2. Sun-photometer measurements

SP data are obtained from AERONET. The SP instrument used by AERONET is the Cimel CE-318 photometer. The data product used is the

Table 1
Instruments and station names considered, grouped by sites (in bold). Position column includes latitude, longitude and height above sea level.

Station (**Site**)	Instrument	Position	Time-span
Evora			
Evora	SP	(38.568 N, 7.912 W, 293 m)	03/07/2003 – present
Evora	MWR	(38.568 N, 7.912 W, 293 m)	20/10/2014 – 05/07/2017 10/07/2018 – present
EVOR	GNSS	(38.568 N, 7.904 W, 299 m)	01/10/2007 – 15/05/2013
SMA1	GNSS	(38.459 N, 7.75 W, 189 m)	14/01/2009 – present
Cascais			
Cabo da Roca	SP	(38.782 N, 9.498 W, 136 m)	10/12/2003 – 24/02/2008 12/03/2010 – present
Cabo Raso	SP	(38.709 N, 9.486 W, 20 m)	26/01/2008 – 01/04/2009
CASC	GNSS	(38.693 N, 9.419 W, 22 m)	19/07/1997 – present
Sagres			
SAGRES	SP	(37.048 N, 8.874 W, 26 m)	29/01/2010 – 14/12/2012
SAGR	GNSS	(37.022 N, 8.960 W, 39 m)	07/01/2008 – 15/05/2013
Azores			
ARM_Graciosa	SP	(39.091 N, 28.029 W, 15 m)	30/09/2013 – present
Graciosa	SP	(39.091 N, 28.030 W, 15 m)	29/04/2009 – 04/01/2011
Graciosa	MWR	(39.92 N, 28.026 W, 30 m)	25/02/2014 – present
AZGR	GNSS	(39.088 N, 28.023 W, 32 m)	26/12/2008 – 10/11/2020
Granada			
Granada	SP	(37.164 N, 3.605 W, 680 m)	29/12/2004 – 22/06/2021
Granada	MWR	(37.164 N, 3.605 W, 680 m)	02/01/2011 – 24/12/2020
GRA1	GNSS	(37.190 N, 3.596 W, 774 m)	17/05/2010 – 29/2022/10

new version 3.0. Regarding data quality, only those data with level 2.0, that is to say, the highest quality, were considered. The AERONET stations selected are shown in Table 1.

SP measures direct solar radiation, so it is necessary that the sun be visible and not covered by clouds to carry out the measurement. The instrument is described in depth in Holben et al. (1998). The retrieval for IWV is based on the Beer–Lambert-Brouger law. The extinction caused by water vapor is obtained by removing the extinction from other sources in a band of high absorption by water vapor. Then, the water vapor transmission is transformed to IWV through the relation studied by Bruegge et al. (1992), Halthore et al. (1992). This technique provides an expectation of a 10% in one-sigma uncertainty in comparison to GNSS IWV (Giles et al., 2019).

2.3. GNSS measurements

Ground-based GNSS stations can retrieve IWV from the zenith total delay (ZTD) that the signal suffers while traveling between the Satellite and the receiver on ground. ZTD is the sum of the zenith hydrostatic delay (ZHD) and zenith wet delay (ZWD), being the latter due exclusively to water vapor (Bevis et al., 1992). This can be converted into IWV through a multiplication factor that is dependent on the mean temperature of the atmosphere weighted by water vapor profile, known as Davis temperature (Davis et al., 1985). The data is processed by Nevada Geodetic Laboratory (Blewitt et al., 2018). The processing of the GNSS data to produce ZTD values is carried out using Jet Propulsion Laboratory's (JPL) GipsyX 1.0 software, which is fed with JPL's Repro 3.0 orbits and clocks data, and Vienna Mapping Function 1 (Boehm et al., 2006, VMF1) gridded data and mapping function parameters. JPL's data and software can be obtained fromhttps://gipsyx.jpl.nasa.gov/. The Davis temperature is obtained from VMF1 gridded numerical weather model data. All this processing is done by Nevada Geodetic Laboratory, delivering a IWV product in their tropospheric files, together with other variables (ZTD, Davis Temperature, and other variables related with the tropospheric correction in GNSS processing). The stations selected and their positions are shown Table 1, while the approximate locations of the sites are shown in Fig. 1.

2.4. Auxiliary data

Some auxiliary data have been used to filter out periods with precipitation from MWR data. Azores and Evora MWR stations counted with precipitation stations with 1-min resolution few meters apart from the MWR station. For Granada MWR station, the daily precipitation data available in the European Climate Assessment (ECA) have been taken, from two stations in the same city (ID 000417 and 003932).

3. Methodology

First, outliers and incorrect data are removed applying some quality control filters, which are detailed here. MWR are known to heavily overestimate water vapor measurements under rainy conditions. Therefore, MWR data not considered when any precipitation occurred. In the case of Granada MWR data, precipitation information at the station was not available. Therefore, daily precipitation data from two nearby stations have been used, filtering out days in which any of the stations reported precipitation. Also, outliers were also removed from all MWR data. For the calculation of outliers, the mean and SD for each day of year were used. Then, data separated from the mean value more than 2 SD were considered as outliers and removed from the data set. Regarding AERONET data, since the level 2.0 was used, which were already cloud-screened and quality-assured data, no further filters were applied. Finally, GNSS with uncertainty over 5% were removed.

The instruments are compared by matching simultaneous data. To accomplish this, the data from MWR and SP are averaged hourly for each instrument and site. Hourly GNSS IWV (XX:00 h) data are taken as the reference, and the difference between the other instruments and the GNSS are calculated, together with relative difference (difference divided by reference GNSS value) linear regression parameters. In the case that more than one station of the same instrument (see Table 1) has data available at coincident site and time, the values are averaged. This occurs in the case of SMA1 and EVOR GNSS stations in Evora site. The dependence of these differences on some parameters (IWV, SZA, seasonal) are analyzed as well. To do so, the statistics (MBE and SD) of the differences are calculated over data binned according to the parameter values. MBE is calculated as the mean of the differences, while the SD as the standard deviation of the differences. The parameters relative mean bias error (rMBE) and relative standard deviation (rSD) are calculated in the same way as MBE and SD, but using the relative differences instead of the differences.

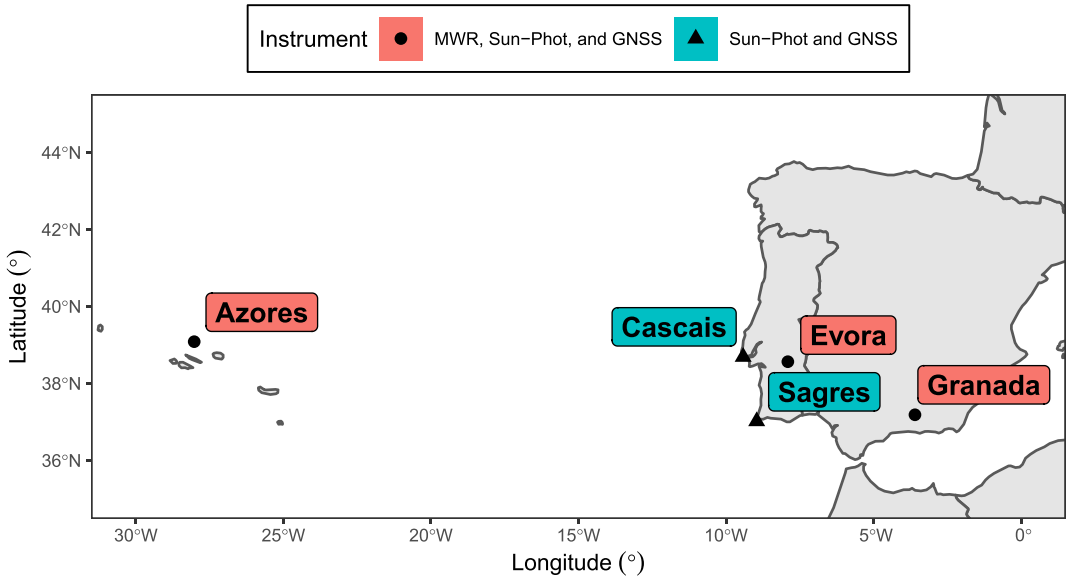

Fig. 1. Map showing the location of the stations selected for the study. For the specific location of each instrument station, see Table 1.

Table 2
General statistics for the comparison. Site-Instr column shows the site and instrument. The IWV column shows the mean GNSS IWV in mm. TS is the time-span in years from 2000. MBE, SD and y_0 are in mm, while rMBE and rSD are in percentage. Slope, R^2 and n are unitless.

Station	TS	IWV	MBE	SD	rMBE	rSD	n	y_0	slope	R^2
MWR										
Azores	14–20	23.22	+0.32	0.98	+1.85	4.83	27605	0.62	0.99	0.98
Evora	14–21	16.29	+1.35	1.21	+9.60	9.01	17852	1.43	1.00	0.96
Granada	11–20	14.60	+1.85	1.11	+14.44	10.49	36271	1.75	1.01	0.96
SP										
Azores	09–20	23.18	−0.64	1.45	−2.19	5.95	5814	1.11	0.92	0.97
Cascais	03–13	17.40	−1.20	1.36	−5.82	7.63	9199	1.27	0.86	0.97
Evora	07–20	16.44	−1.05	1.37	−5.54	7.76	22974	0.92	0.88	0.96
Granada	10–21	14.91	−0.07	1.29	+0.31	22.29	20982	0.94	0.93	0.94
Sagres	10–12	18.47	−1.30	1.10	−6.75	5.52	2320	0.50	0.90	0.97

4. Results and discussion

4.1. General statistics

Table 2 shows the MBE and SD of both differences and relative differences between the MWR/SP and GNSS. It is observed that all measurements agree very well in general. The results GNSS vs SP are in agreement with Pérez-Ramírez et al. (2014), where these two instruments were compared in several stations worldwide. SP generally show dry biases with MBE below −1.3 mm and rMBE values below −6.75% for all the stations. The lack of bias in the case of Granada SP is noteworthy (MBE of −0.07 mm; 0.31% in terms of rMBE). On the contrary, MWR shows a wet bias of 1.2 mm (8.6%) on average. SD are similar in both instruments, around 1.2 mm (9.0%). SD from SP are below 1.5 mm, while rSD falls below 8.0% in all sites except Granada, with 22.3%.

A linear regression analysis between the IWV from GNSS (independent variable) and the ones from the other instruments (dependent variable) was performed. The relevant parameters are depicted in Table 2, revealing that all intercepts are positive, while all slopes are below the unit. This underestimation of the IWV from GNSS is due to its low sensitivity under low IWV values (Schneider et al., 2010; Van Malderen et al., 2014). Despite this fact, the coefficient of determination (R^2) shows a very high correlation (0.94 to 0.98) in all cases.

4.2. Dependence with IWV

The dependence of the differences on IWV is studied through Fig. 2. In it, co-located pairs of IWV are grouped in bins of 5 mm of GNSS IWV. The MBE and SD statistics are calculated over these bins and represented against IWV. It is shown that both indices worsen as IWV increases. MBE linearly increases for MWR (wet bias), while it linearly decreases for SP (dry bias, negative MBE). The rate of change is, however, very different among the different stations and instruments, and no pattern seems to arise. The slope of MBE change can be as steep as −0.12 (Cascais SP), or as flat as 0.003 (Granada SP). Here, we highlight the lack of bias between SP and GNSS in Granada station for all the bins. Of course, as these changes are rather small in comparison with the total IWV range, the rMBE would show an opposite behavior, decreasing as IWV increases. Very similar results were obtained for other set of Spanish stations in Vaquero-Martínez et al. (2022), and also these results are consistent with those by Fragkos et al. (2019) in a Romanian station. Pérez-Ramírez et al. (2014) noted that differences of SP with other instruments (MWR, GNSS and radiosondes) became larger as IWV increased consistently with a constant percentage difference of around ∼5% (5.3% for GNSS). SD increases as IWV increases in all cases. Again, despite the linearity of the relation SD–IWV, the slope is very different among the instruments and stations. SD–IWV slopes are in the range 0.02 to 0.07.

4.3. Dependence with SZA

The SZA is expected to disturb the measurements, as the geometry is fundamental in SP: the instrument points to the sun for measurements. Therefore, low SZA values imply higher levels of short-wave radiation, allowing the SP to have higher quality measurements. In that scenario, it is advantageous that the observed water vapor column will be closer to the vertical column, so the conversion from slant to vertical column water vapor is easier. Hence, it is expected that SP IWV shows worse performance for high SZA. However, other aspects can be considered in the opposite direction: increased SZA implies a larger optical path for water vapor, increasing the sensibility of the instrument, specially under dry conditions. This a controversial issue and probably dependent on specific situations. In contrast, MWR and GNSS are not expected to be influenced by SZA as they do not rely on solar radiation for their water vapor retrieval.

Fig. 3 shows MBE and SD in 15° bins. MWR shows some slight tendency to decrease MBE with SZA, except in Azores. As for SP, although it does not show a very strong trend, some of the higher SZA bins show increased dry bias (more negative MBE). Similar results, with stronger negative bias for SZA larger than 70°, were also found in Vaquero-Martínez et al. (2022), Fragkos et al. (2019). It is worth to note that the effect is generally more marked for humid situations (IWV over 20 mm). SD decreases with SZA in the case of low IWV for MWR. The SD for SP measurements shows an interesting behavior along the SZA bins. In the range 30° to 60°, there is a minimum. Therefore, very low SZA bins show higher SD. In any case, it must be noted that the changes in SD due to SZA are much smaller than the ones due to IWV (see Fig. 2, bottom).

4.4. Seasonal dependence

The aforementioned influential factors typically have seasonal patterns. Therefore, it is likely that the statistical indices under study show a seasonal dependence. Fig. 4 shows the MBE and SD values along the months of the year for the complete data-set and for the low IWV and high IWV subsets. MBE does not show a marked pattern in the case of MWR–GNSS differences. However, SP shows more or less marked patterns depending on the stations. Sagres, Cascais and Evora show strong seasonal dependencies (difference between maximum and minimum MBE above 1 mm), while Granada and Azores have weaker dependencies. Generally, MBE takes stronger negative values at summer months and less negative (or positive) in winter. SD seasonal dependence is also more marked in the case of SP than MWR. Summer values have, in general, larger SD values than winter. This behavior of increased discrepancies in summer is probably related to higher IWV values in this season, and as shown in Section 4.2, since IWV seems to be the most influential factor in SP performance.

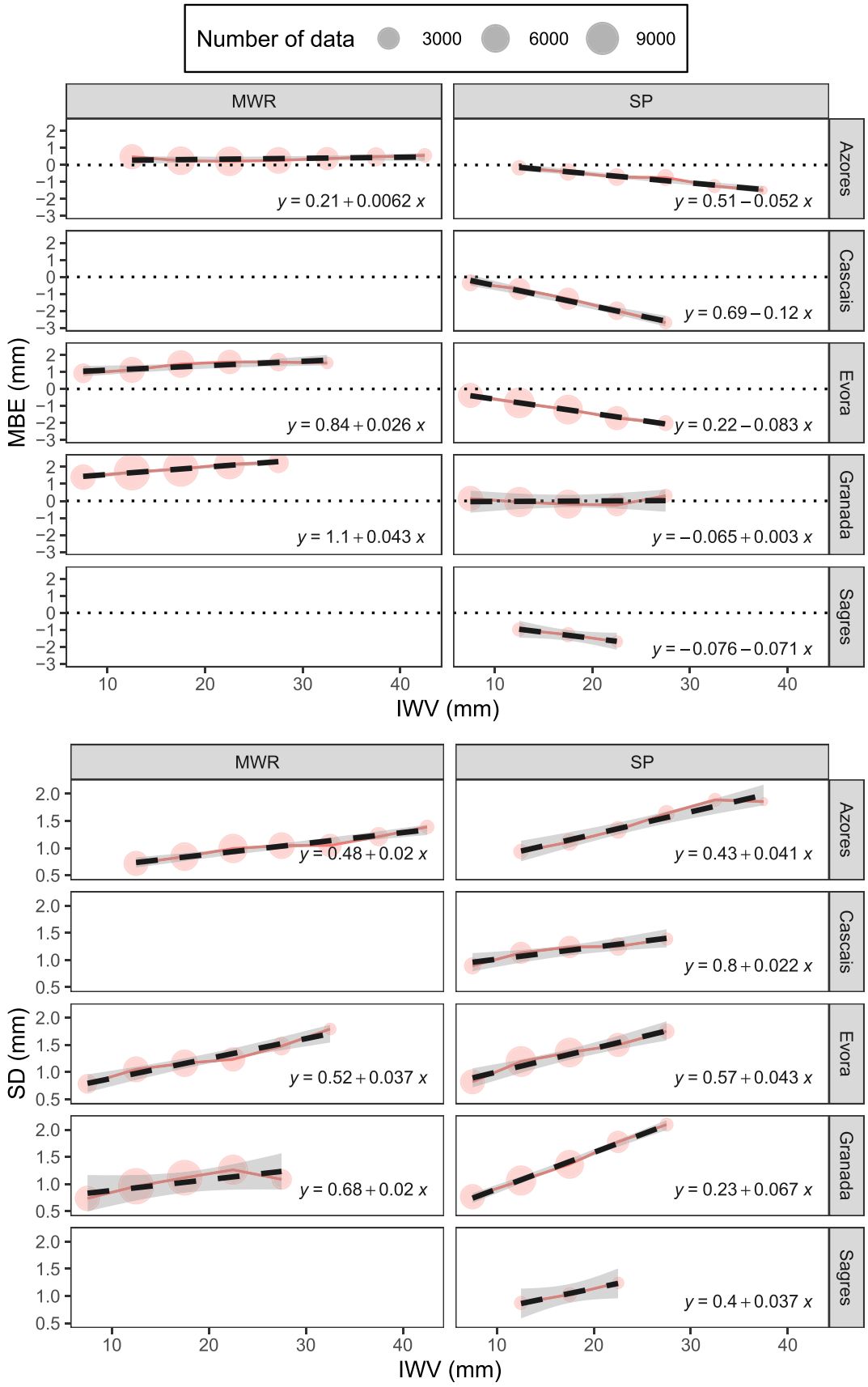

Fig. 2. MBE (top panel) and SD (bottom panel) evolution along the GNSS IWV bins of 5 mm.

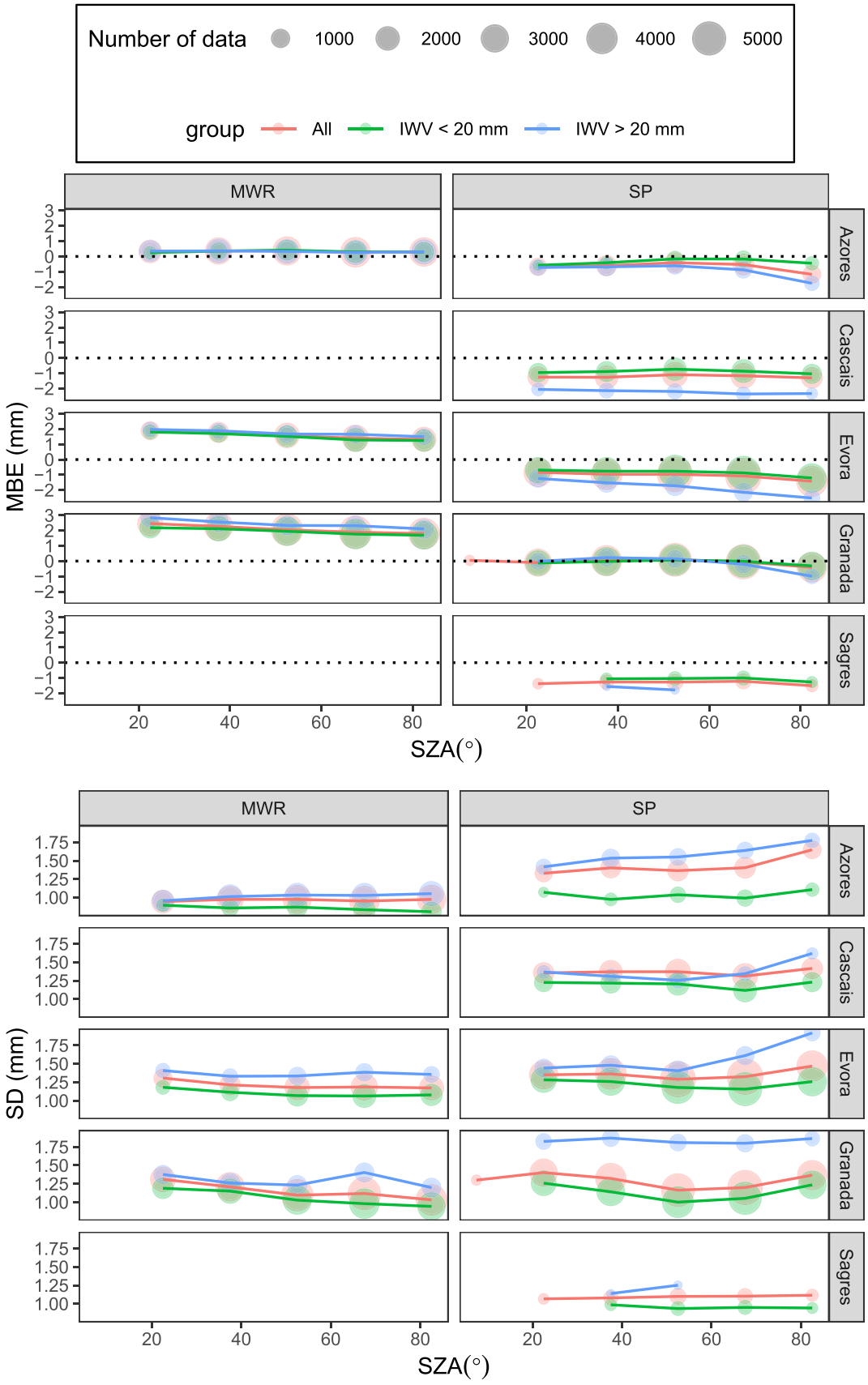

Fig. 3. MBE (top panel) and SD (bottom panel) evolution along the GNSS SZA bins of 15°.

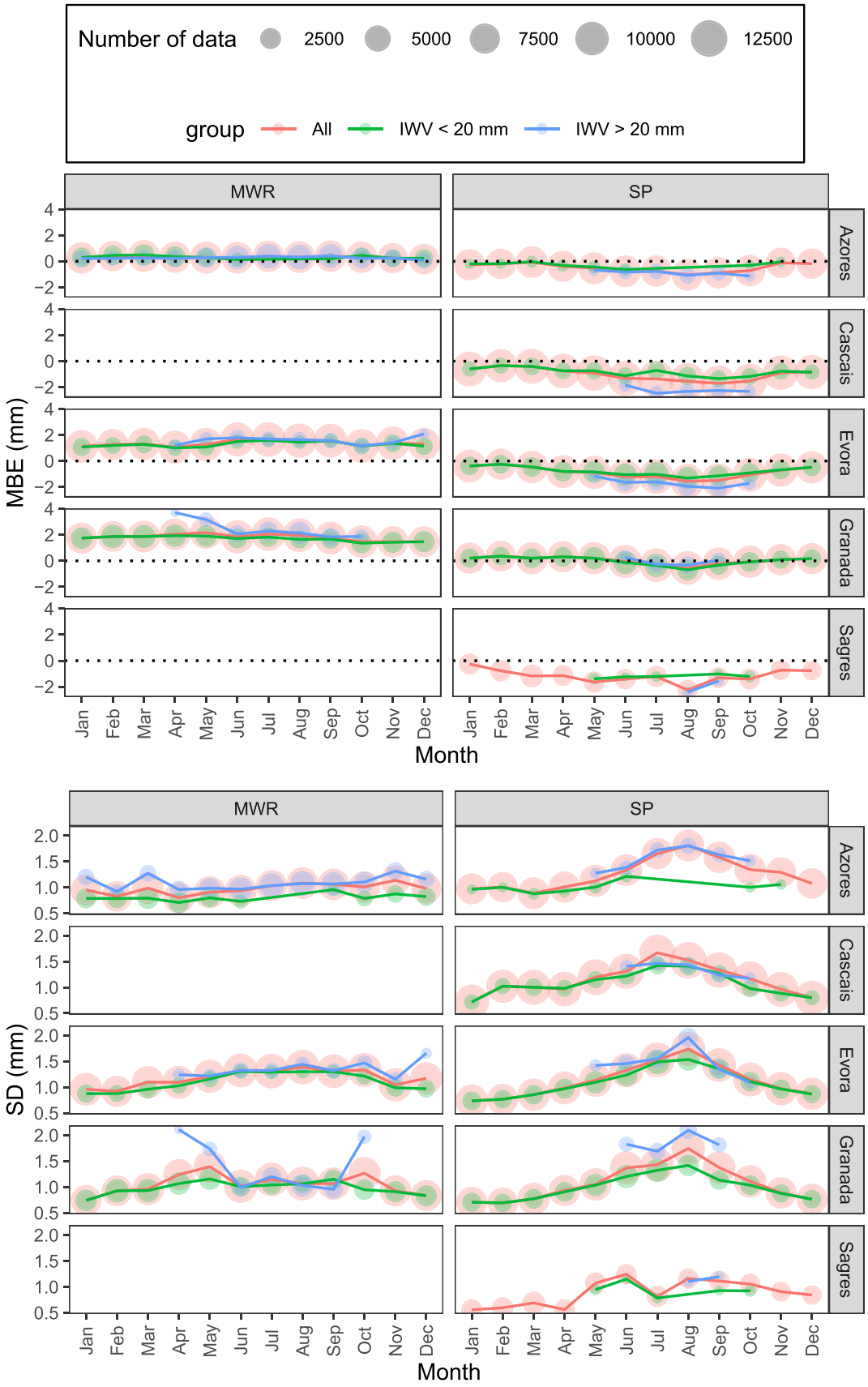

Fig. 4. MBE (top panel) and SD (bottom panel) evolution along the year.

5. Conclusion

IWV data recorded from MWR and SP exhibit an excellent agreement against reference GNSS IWV data in the Portuguese and Spanish stations analyzed. The correlation coefficient is very high in all cases (R^2 between 0.94 and 0.98). Also, SD values are always below 1.5 mm. In general, MWR show larger values (wet bias) while SP exhibit lower values (dry bias) of IWV with respect to the reference GNSS measurements. A strong dependence of both MBE and SD on IWV has been observed for both the MWR (wet bias) and SP (dry bias) IWV with respect to GNSS. Both indices, MBE and SD show linear behavior, but the slopes are site- and instrument-dependent. SZA dependence was also studied and it was found that MWR slightly decrease MBE as SZA increases, with the only exception of Azores site. However, SP showed very weak changes with SZA except in the case of the higher SZA bins (stronger negative MBE), with a stronger effect in humid situations. Finally, the seasonal dependence was also analyzed, and it was found to be modulated mainly by the IWV dependence. Therefore, larger discrepancies are found in summer months, when the IWV is higher. Nevertheless, MBE seasonal cycle was quite weak in the case of MWR vs GNSS differences, while more marked for SP.

In summary, both MWR and SP showed a very good agreement with GNSS. The observed dependencies with IWV must be taken into account, since they have been the most important factor in inter-instrument differences. It is also fundamental to filter out situations that can compromise the quality of the instruments (rainfall situations in MWR, for example).

CRediT authorship contribution statement

Javier Vaquero-Martínez: Formal-analysis, Methodology, Software, Visualization, Writing-original-draft, Writing-review-editing. **Manuel Antón:** Conceptualization, Methodology, Project-administration, Supervision, Resources, Writing-review-editing. **Maria João Costa:** Data-curation, Supervision, Resources, Funding-acquisition, Writing-review-editing. **Daniele Bortoli:** Data-curation, Supervision, Resources. **Francisco Navas-Guzmán:** Data-curation, Supervision, Funding-acquisition, Writing-review-editing. **Lucas Alados-Arboledas:** Data-curation, Supervision, Resources.

Declaration of Competing Interest

The authors declare that they have no known competing financial interests or personal relationships that could have appeared to influence the work reported in this paper.

Data availability

Data will be made available on request.

Acknowledgments

The work is co-funded by Portuguese national funds through FCT–Fundação para a Ciência e Tecnologia, I.P., in the framework of the ICT project with the references UIDB/04683/2020 and UIDP/04683/2020, as well as TOMAQAPA project (PTDC/CTAMET/29678/2017). Francisco Navas-Guzmán received funding from the Ramón y Cajal program (ref. RYC2019-027519-I) of the Spanish Ministry of Science and Innovation. Work at Granada was also supported by Grant PID2021-128008OB-I00 funded by MCIN/AEI/10.13039/501100011033/FEDER "A way of making Europe", and by the European Union's Horizon 2020 research and innovation program through projects ACTRIS.IMP (grant agreement No 871115) and ATMO_ACCESS (grant agreement No 101008004), by the Spanish Ministry of Science and Innovation through project ELPIS (PID2020-120015RB-I00), by Junta de Andalucía AERO-PRE (P-18-RT-3820). ENA Data were obtained from the Atmospheric Radiation Measurement (ARM) Program sponsored by the U.S. Department of Energy, Office of Science, Office of Biological and Environmental Research, Climate and Environmental Sciences Division. We thank the AERONET PI(s) and Co-I(s) and their staff for establishing and maintaining the sites used in this investigation.

References

Bevis, M., Businger, S., Herring, T.A., Rocken, C., Anthes, R.A., Ware, R.H., 1992. GPS meteorology: Remote sensing of atmospheric water vapor using the global positioning system. J. Geophys. Res. 97, 15787. https://doi.org/10.1029/92JD01517.

Blewitt, G., Hammond, W., Kreemer, C., 2018. Harnessing the GPS Data Explosion for Interdisciplinary Science. Eos 99. https://doi.org/10.1029/2018EO104623.

Boehm, J., Werl, B., Schuh, H., 2006. Troposphere mapping functions for GPS and very long baseline interferometry from European Centre for Medium-Range Weather Forecasts operational analysis data: TROPOSPHERE MAPPING FUNCTIONS FROM ECMWF. J. Geophys. Res.: Solid Earth 111. https://doi.org/10.1029/2005JB003629 n/a–n/a.

Bruegge, C.J., Conel, J.E., Green, R.O., Margolis, J.S., Holm, R.G., Toon, G., 1992. Water vapor column abundance retrievals during FIFE. J. Geophys. Res. 97, 18759. https://doi.org/10.1029/92JD01050.

Cadeddu, M., 2021. Microwave Radiometer – 3-Channel (MWR3C) Instrument Handbook. Technical Report DOE/SC-ARM/TR-108, 1039668. doi:10.2172/1039668.

Cadeddu, M.P., Liljegren, J.C., Turner, D.D., 2013. The Atmospheric radiation measurement (ARM) program network of microwave radiometers: Instrumentation, data, and retrievals. Atmos. Meas. Tech. 6, 2359–2372. https://doi.org/10.5194/amt-6-2359-2013.

Colman, R., 2003. A comparison of climate feedbacks in general circulation models. Clim. Dyn. 20, 865–873. https://doi.org/10.1007/s00382-003-0310-z.

Colman, R.A., 2015. Climate radiative feedbacks and adjustments at the Earth's surface. J. Geophys. Res.: Atmos. 120, 3173–3182. https://doi.org/10.1002/2014JD022896.

Crewell, S., Lohnert, U., 2007. Accuracy of Boundary Layer Temperature Profiles Retrieved With Multifrequency Multiangle Microwave Radiometry. IEEE Trans. Geosci. Remote Sens. 45, 2195–2201. https://doi.org/10.1109/TGRS.2006.888434.

Davis, J.L., Herring, T.A., Shapiro, I.I., Rogers, A.E.E., Elgered, G., 1985. Geodesy by radio interferometry: Effects of atmospheric modeling errors on estimates of baseline length. Radio Sci. 20, 1593–1607. https://doi.org/10.1029/RS020i006p01593.

Fragkos, K., Antonescu, B., Giles, D.M., Ene, D., Boldeanu, M., Efstathiou, G.A., Belegante, L., Nicolae, D., 2019. Assessment of the total precipitable water from a sun photometer, microwave radiometer and radiosondes at a continental site in southeastern Europe. Atmos. Meas. Tech. 12, 1979–1997. https://doi.org/10.5194/amt-12-1979-2019.

Giles, D.M., Sinyuk, A., Sorokin, M.G., Schafer, J.S., Smirnov, A., Slutsker, I., Eck, T.F., Holben, B.N., Lewis, J.R., Campbell, J.R., Welton, E.J., Korkin, S.V., Lyapustin, A.I., 2019. Advancements in the Aerosol Robotic Network (AERONET) Version 3 database – automated near-real-time quality control algorithm with improved cloud screening for Sun photometer aerosol optical depth (AOD) measurements. Atmos. Meas. Tech. 12, 169–209. https://doi.org/10.5194/amt-12-169-2019.

Halthore, R., Markham, B., Deering, D., 1992. Atmospheric Correction and Calibration During Kurex-91. In: [Proceedings] IGARSS '92 International Geoscience and Remote Sensing Symposium, vol. 2. IEEE, Houston, TX, pp. 1278–1280. https://doi.org/10.1109/IGARSS.1992.578413.

Holben, B., Eck, T., Slutsker, I., Tanré, D., Buis, J., Setzer, A., Vermote, E., Reagan, J., Kaufman, Y., Nakajima, T., Lavenu, F., Jankowiak, I., Smirnov, A., 1998. AERONET—A Federated Instrument Network and Data Archive for Aerosol Characterization. Remote Sens. Environ. 66, 1–16. https://doi.org/10.1016/S0034-4257(98)00031-5.

Löhnert, U., Crewell, S., 2003. Accuracy of cloud liquid water path from ground-based microwave radiometry 1. Dependency on cloud model statistics: CLOUD LIQUID WATER RETRIEVAL. Radio Sci. 38 https://doi.org/10.1029/2002RS002654 n/a–n/a.

Myhre, G., Shindell, D., Bréon, F.-M., Collins, W., Fuglestvedt, J., Huang, J., Koch, D., Lamarque, J.-F., Lee, D., Mendoza, B., Nakajima, T., Robock, A., Stephens, G., Takemura, T., Zhang, H., 2013. Anthropogenic and Natural Radiative Forcing. In: Climate Change 2013: The Physical Science Basis. Contribution of Working Group I to the Fifth Assessment Report of the Intergovernmental Panel on Climate Change, Ipcc ed. Cambridge University Press, pp. 659–740.

Pérez-Ramírez, D., Whiteman, D.N., Smirnov, A., Lyamani, H., Holben, B.N., Pinker, R., Andrade, M., Alados-Arboledas, L., 2014. Evaluation of AERONET precipitable water vapor versus microwave radiometry, GPS, and radiosondes at ARM sites. J. Geophys. Res.: Atmos. 119, 9596–9613. https://doi.org/10.1002/2014JD021730.

Rose, T., Crewell, S., Löhnert, U., Simmer, C., 2005. A network suitable microwave radiometer for operational monitoring of the cloudy atmosphere. Atmos. Res. 75, 183–200. https://doi.org/10.1016/j.atmosres.2004.12.005.

Schneider, M., Romero, P.M., Hase, F., Blumenstock, T., Cuevas, E., Ramos, R., 2010. Continuous quality assessment of atmospheric water vapour measurement techniques: FTIR, Cimel, MFRSR, GPS, and Vaisala RS92. Atmos. Meas. Tech. 3, 323–338. https://doi.org/10.5194/amt-3-323-2010.

Sinyuk, A., Holben, B.N., Eck, T.F., Giles, D.M., Slutsker, I., Korkin, S., Schafer, J.S., Smirnov, A., Sorokin, M., Lyapustin, A., 2020. The AERONET Version 3 aerosol retrieval algorithm, associated uncertainties and comparisons to Version 2. Atmos. Meas. Tech. 13, 3375–3411. https://doi.org/10.5194/amt-13-3375-2020.

Turner, D.D., Clough, S.A., Liljegren, J.C., Clothiaux, E.E., Cady-Pereira, K.E., Gaustad, K. L., 2007. Retrieving Liquid Wat0er Path and Precipitable Water Vapor From the Atmospheric Radiation Measurement (ARM) Microwave Radiometers. IEEE Trans. Geosci. Remote Sens. 45, 3680–3690. https://doi.org/10.1109/TGRS.2007.903703.

Van Malderen, R., Brenot, H., Pottiaux, E., Beirle, S., Hermans, C., De Mazière, M., Wagner, T., De Backer, H., Bruyninx, C., 2014. A multi-site intercomparison of integrated water vapour observations for climate change analysis. Atmos. Meas. Tech. 7, 2487–2512. https://doi.org/10.5194/amt-7-2487-2014.

Vaquero-Martínez, J., Antón, M., 2021. Review on the Role of GNSS Meteorology in Monitoring Water Vapor for Atmospheric Physics. Remote Sens. 13, 2287. https://doi.org/10.3390/rs13122287.

Vaquero-Martínez, J., Bagorrilha, A.F., Antón, M., Antuña-Marrero, J.C., Cachorro, V.E., 2022. Comparison of CIMEL sun-photometer and ground-based GNSS integrated water vapor over south-western European sites. Atmos. Res. 275, 106217 https://doi.org/10.1016/j.atmosres.2022.106217.

Yu, C., Li, Z., Blewitt, G., 2021. Global Comparisons of ERA5 and the Operational HRES Tropospheric Delay and Water Vapor Products With GPS and MODIS. Earth Space Sci. 8 https://doi.org/10.1029/2020EA001417.